

(relative to year 2000 levels) (31). While it is recognized that limiting global warming to 1.5 °C could also be beneficial for human health, a fundamental unknown is the impact upon dengue fever. Here, we use a multi-GCM, multisenario approach to investigate and quantify the risks avoided by limiting global-mean temperature to 1.5 °C above preindustrial levels compared with that occurring at 2 °C or 3.7 °C. Using the ClimGen pattern-scaling tool (32), we generated climate projections from five Coupled Model Intercomparison Project Phase 5 (CMIP5) climate models (33). We scaled the simulated patterns of climate change of each model, using the Integrated Model to Assess the Global Environment (IMAGE) modeling framework, which identifies socioeconomic pathways and projects the climatic implications of different climate and energy policy scenarios (34). Specifically, we investigated a business-as-usual scenario where global-mean temperature rises by 3.7 °C by 2100. We compared this scenario with two alternative scenarios where, due to mitigation strategies, there is a 66% probability of holding global-mean temperature increase below 1.5 °C and 2.0 °C.

We quantified the likely number of dengue cases and changes in the length of the dengue transmission season for the period 1961–1990 and for each of the three scenarios for the periods 2040–2069 (2050s) and 2086–2115 (2100). The estimated number of cases was computed using clinical and laboratory-confirmed dengue reports for the three most populated countries in LATAM (Brazil, Colombia, and Mexico) and fitting a climate-driven empirical model of dengue incidence that accounts for long-term and seasonal trends (35) and whose structure and climatic parameters were selected using time-series cross-validation (TSCV) (36) so that the model captured the spatial and temporal variations in observed dengue data.

Results

We fitted different model specifications for our empirical dengue model, regressing the dengue data for Brazil, Colombia, and Mexico with all possible combinations of climatic predictors using TSCV (*Materials and Methods*). The lowest mean absolute error (MAE = 103 cases per month) was achieved with a negative binomial generalized additive mixed model (GAMM) including temperature lagged 0–2 mo ($T_{0:2}$) and potential evapotranspiration (PET) lagged 0–2 mo ($PET_{0:2}$) as climatic covariates. That model was selected for projecting the potential impacts of climate change. The model output captures well the observed temporal trends on dengue transmission in the three countries with most observed reports falling within the confidence intervals (*SI Appendix, Fig. S1*). The country-specific MAE estimates were 99, 48, and 188 monthly dengue cases for Brazil, Colombia, and Mexico, respectively.

The effects of future climate on the population at risk for dengue for the multimodel ensemble mean were then projected for LATAM from Mexico to northern Argentina and are summarized in Table 1. We averaged the mean predicted number of cases across all climate change scenarios and compared them with the baseline (*SI Appendix, Fig. S2*). The number of dengue cases for the 2050s period was, on average, 260% larger than the 1961–1990 baseline scenario with about 6.9 million extra cases

Table 1. Multi-GCM ensemble mean (and range) of the predicted number of dengue cases (million cases per year) in LATAM under different climate change scenarios

Scenario	Baseline	2050s	2100
1.5 °C	4.3 (3.0–6.1)	10.7 (7.0–16.7)	8.8 (5.9–13.6)
2.0 °C		11.0 (7.1–17.2)	9.3 (6.1–14.7)
3.7 °C		11.8 (7.4–19.2)	12.1 (6.9–22.1)

The baseline values are the same for all climate change scenarios.

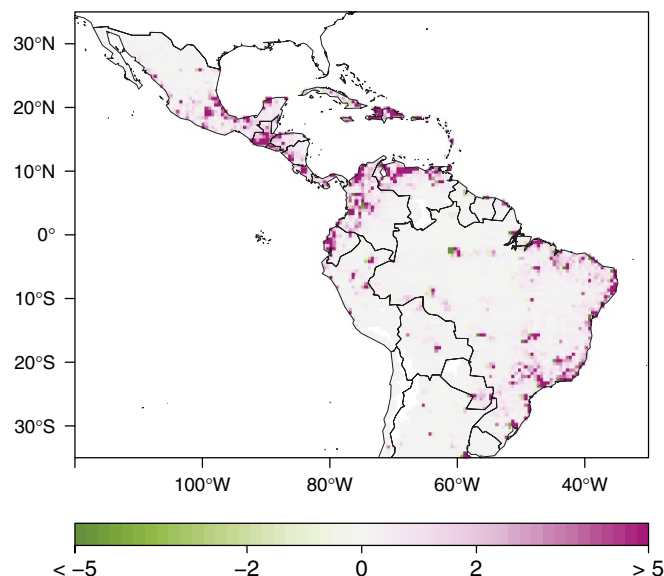


Fig. 1. Multi-GCM ensemble mean of the predicted additional (to the predicted number of cases for the 1961–1990 baseline) number of dengue cases under a 1.5 °C scenario for the 2050s period (thousands).

per year. A 234% average increase was estimated for the 2100 period with 5.8 million extra cases per year. We note that the population at risk for dengue is estimated to be lower by the end of the century, but only for the 1.5 °C and 2.0 °C scenarios.

Critically, we show that limiting global warming to about 2.0 °C above preindustrial levels could reduce the number of dengue cases by ~0.8 (0.3–2.0) million cases per year compared with a no-policy scenario with a 3.7 °C warming for the 2050s period and by ~2.8 (0.8–7.4) million cases per year for the 2100 period. Constraining global warming to 1.5 °C produces an additional drop in dengue cases of ~0.3 (0.1–0.5) million avoided cases by the middle of the century and ~0.5 (0.2–1.1) million avoided cases by the end of the century. It is important to note that when comparing the 3.7 °C scenario with the 1.5 °C scenario, the estimated benefit by the end of the century corresponds to ~77% (25–200%) of the estimated mean number of cases for the baseline period (1961–1990).

Fig. 1 highlights the areas likely to experience significant changes in the expected number of dengue cases under the 1.5 °C scenario for the 2050s period. We note that southern Mexico, many Caribbean Island states, northern Ecuador, Colombia, Venezuela, and the coastal Brazilian states will be most affected by increases in dengue cases. Similar geographical patterns were observed under the 2.0 °C and 3.7 °C scenarios both for the 2050s and the 2100 periods.

Table 2 presents the difference in the predicted number of cases per country, comparing the 3.7 °C scenario to the 1.5 °C scenario. It is noted that Brazil will benefit the most from limiting global warming to 1.5 °C with an estimated 0.5 (0.2–1.0) million avoided cases per year by the 2050s and 1.4 (0.5–3.1) million avoided cases by 2100. The benefit in disease burden in the 2050s period is over five times the estimated absolute benefit in dengue cases for Colombia which we project to be the second most benefited country in the region. Except for Argentina, the countries with the largest benefits are also the countries with some of the largest dengue incidences in the region (16).

Fig. 2 depicts the changes in the length of the dengue transmission season (LTS) compared against the baseline scenario. Fig. 2 shows that the areas experiencing increases in LTS of more than 3 mo show considerably lower increase if warming is constrained to 1.5 °C compared with a 3.7 °C warming scenario. Such

regions, possibly due to lower environmental suitability for *A. aegypti* as estimated by ref. 22. We note that lower temperatures increase the development time and gonotrophic cycle of the vector, decrease its biting rate, and reduce its ability for transmitting the virus to a human host, reducing disease transmission (12, 42).

In this study we show that reductions in warming from 3.7 °C to 2.0 °C or 1.5 °C above preindustrial levels may result in important health benefits although the estimated number of cases will still be above current levels. Specifically, we predict that limiting warming to 1.5 °C will reduce the estimated number of dengue cases by 0.3 (0.1–0.5) million toward the middle of the century and by 0.5 (0.2–1.1) million by the end of the century compared with a scenario projected to reach 2.0 °C of global-mean warming by 2100. Moreover, limiting warming to 1.5 °C will reduce the expected number of cases by 1.1 (0.4–2.5) million by the 2050s and by 3.3 (1.0–8.5) million by 2100 compared with a scenario where global-mean temperature warms 3.7 °C. Thus, our findings emphasize that holding the increase in global-mean temperature at about 1.5 °C above preindustrial levels may significantly reduce public health risks.

Although our spatially explicit projections of dengue risk provide useful information for public health preparedness, there are some caveats. First, our results have not considered the mass deployment of a vaccine which would significantly reduce the risk of infection. Recent studies suggest that a tetravalent dengue vaccine is efficacious against virologically confirmed dengue cases (43, 44). However, the evaluation of this tetravalent vaccine indicates that its mean efficacy is only about 58% with some variation between serotypes (45). Second, we have based our risk estimates on one of the most comprehensive dengue datasets yet assembled. Still, other determinants of disease such as socioeconomic development, intervention deployment, urbanization, and the international movement of people and goods, not explicitly accounted for in our model, may produce significant changes in the levels of risk experienced by the affected populations (21, 26, 37). Importantly, to this date there are no publicly available continuous, gridded socioeconomic data for the contemporary and future periods that could be incorporated into such modeling exercises. This situation highlights the need for the development of such socioeconomic datasets (46). Third, the quality of surveillance systems is likely to vary widely between and within countries, adding uncertainty to our estimates. To our knowledge, there are no available studies or datasets quantifying between- or within-country variation in surveillance data quality. Thus, while we adopted a GAMM approach (*Materials and Methods*) to control for those effects, we highlight the need for further quantifying the quality of epidemiological surveillance data.

Materials and Methods

Dengue Surveillance Data. Monthly laboratory-confirmed dengue reports were obtained from the Colombian (portalsivigila.ins.gov.co/sivigila/documentos/Docs.1.php) and Mexican (www.epidemiologia.salud.gob.mx/anuario/html/anuarios.html) Ministries of Health while suspected (clinical) reports were obtained from the Brazilian Ministry of Health (tabnet.datasus.gov.br/cgi/deftohtm.exe?sinanwin/cnv/denguebr.def). Data from Mexico and Brazil were obtained for the period January 2001 to December 2012, while Colombian data were retrieved for the period January 2007 to December 2012. Colombian data were retrieved at the department level ($n = 32$), Mexican data at the state level ($n = 32$), and Brazilian data at the municipal county level ($n = 5566$). The Brazilian municipal counties are considerably smaller in area and population than the Colombian departments or the Mexican states, and their data were characterized by low case counts. The Brazilian municipal counties were consequently aggregated into larger geographical units by dividing their centroid coordinates into 286 latitude–longitude intervals and merging all counties with centroid coordinates within each bin together. Missing dengue counts were imputed for areas with less than 20% missing values using a singular value decomposition-based method (47), included in the *bcv* package (48) for R (49). Areas with over 20% missing counts ($n = 4,177$) were removed.

Climate Observations. Gridded monthly mean temperature (°C), total precipitation (mm·mo^{−1}), and potential evapotranspiration (mm·mo^{−1}) data were obtained from the Climatic Research Unit (CRU) TS3.24 climate archives (crudata.uea.ac.uk/cru/data/hrg/) at a 0.5° × 0.5° resolution for land cells only for the period January 2001 to December 2012 (50). Three-month moving averages of mean temperature, total precipitation, and potential evapotranspiration were used as predictors to account for the delayed effects of climate on dengue incidence (9). These were obtained for each administrative unit using the *extract* method included in the R (49) *raster* package (51).

Climate Change Projection Data. Future climate data were derived for a single “middle-of-the-road” shared socioeconomic pathway (SSP2) and for three different global temperature change scenarios developed using the IMAGE modeling framework (34). The first scenario assumes that no additional (to the Cancun pledges) climate policy takes place and, under those conditions, IMAGE simulates global-mean temperature rising to 3.7 °C above preindustrial levels by 2100. The second and third scenarios, on the other hand, assume stringent mitigation strategies to obtain a 66% probability that global-mean temperature will remain below 1.5 °C and 2.0 °C, respectively. For each of these three scenarios, gridded climate data were generated for three 30-y time slices (2040–2069 and 2086–2115 as well as observed climate data for 1961–1990) by scaling patterns of climate change by the global temperature change. The climate change patterns were diagnosed from CMIP5 (33) climate model simulations for use in the ClimGen pattern-scaling tool (32). We selected the same five CMIP5 models as used previously by the Inter-Sectoral Impact Model Intercomparison Project fast-track project to sample a wide range of potential climate changes: Hadley Global Environment Model 2 - Earth System (HadGEM2-ES), Institut Pierre Simon Laplace Coupled Model Version Five A - Low Resolution (IPSL-CM5A-LR), an atmospheric chemistry version of the Model for Interdisciplinary Research on Climate Earth System Model (MIROC-ESM-CHEM), Geophysical Fluid Dynamics Laboratory Earth System Model with MOM, version 4 component (GFDL-ESM2M), and the Norwegian Earth System Model (NorESM1-M) (6, 33). The scaled climate change patterns were combined with the CRU TS (50) observed baseline climate on a 0.5° latitude–longitude grid and with CRU TS observed monthly variability. A notable modification to this standard pattern-scaling approach is that the monthly precipitation variability is also perturbed according to the changes in precipitation variability simulated by each of the five climate models used here, thus representing increases or decreases in future precipitation variance and distribution skewness (32). Projections were generated for monthly mean temperature and precipitation and also for mean minimum and maximum temperatures, cloud cover, and vapor pressure from which PET was calculated using the Penman–Monteith method.

Historic Population Data. Global gridded total population counts were retrieved at a 2.5-arcmin resolution from the Gridded Population of the World project (sedac.ciesin.columbia.edu/data/collection/gpw-v3/about-us) at 5-y intervals for the period 2000–2010. Population data were aggregated at a 0.5° × 0.5° resolution using the Climate Data Operators software (52) for consistency with the climate data. Total population estimates were scaled to agree with the United Nations World Population Prospects yearly population estimates (<http://esa.un.org/unpd/wpp/Download/Standard/Fertility/>). Monthly estimates for each grid box were derived using linear interpolation (6, 9). The estimated population for each geographical unit included in the study was then calculated using the *extract* method included in the R (49) *raster* package (51).

Future Population Scenario Data. Global-scale, spatially explicit population projections consistent with the new SSPs (53) were used to estimate the future population at risk for dengue transmission. We used the SSP2 population scenario, which projects moderate population density and change compared with the other scenarios (53). Data were obtained at 10-y intervals for the period 2010–2100 at a 0.5° × 0.5° resolution.

Model Specification. We obtained more than one dengue observation per geographical area violating the assumption of independence of standard regression models (54). Also, we expect each area to vary independently from other areas in the model due to climatic and nonclimatic determinants of dengue (26, 39). Mixed models provide a solution to the correlated within-area errors by allowing each area to have its own intercept and slope (54). Consequently, the expected number of dengue reports $E(Y_{it})$ for region $i = 1, \dots, I$ at time $t = 1, \dots, T$ was modeled using a GAMM.

Negative binomial and quasi-maximum-likelihood Poisson models were fitted to investigate possible overdispersion in the data. The model specification with the lowest dispersion parameter and the lowest MAE was selected. The general algebraic definition of the models is given by

$$\text{Log}(\mu_{it}) = \eta_{it}$$

$$\eta_{it} = \alpha + \text{Log}(N_{it}) + t' + \sum_{p=1}^P g(x_{it}) + d_i,$$

where η_{it} is a logarithmic link function of the expectation $E(Y_{it} \equiv \mu_{it})$, and Y_{it} is the time series of monthly dengue reports. The term α denotes the intercept; $\text{Log}(N_{it})$ is the logarithm of the population at risk (N) for region i and time t included as an offset to normalize the dengue data by population. Long-term and seasonal trends are controlled for using a time-stratified model including an indicator variable for each year and month (t') (35). The term $g(x_{it})$ denotes the smoothed and delayed relationships between the climatic predictors and dengue incidence defined by thin-plate splines (55). Area-specific random effects (d_i) were included to account for the effects of unknown or unobserved variables in the model such as mosquito control measures.

Best Subset of Climatic Predictors. The best subset of climatic predictors producing the lowest prediction error was defined using a TSCV algorithm (36). Models were fitted using all climatic predictors in isolation, as well as all their possible combinations. Thus, we iteratively fitted all possible models containing one climatic predictor, then two climatic predictors, and so on, until all climatic predictors were included in a single model. The accuracy of each model was evaluated, calculating their MAE.

Training and test sets were created to implement the TSCV. The initial training set comprised 90% of the total number of observations ($n = 144$) per region. At each time step (k), a further observation per region was added to the training set. Consequently, at time step $k = 1$, the training set comprised observations for month $t = 1, \dots, 130$; at $k = 2$ it comprised observations for $t = 2, \dots, 131$, and so on until the training set contained the observations for

$t = n - 1$, where n is the total number of months in the dataset. The test set contained the first observation for each region immediately after the last observation in the training set. Thus, at time step $k = 1$, the test set contained all observations for $t = 131$; at $k = 2$, it contained all observations for $t = 132$, and so on until the test set contained the observations for month $t = n$. We calculated the MAE at each time step $k = 1, \dots, K$, and for each subset of climatic predictors $h = 1, \dots, H$ as in the following matrix:

$$\text{MAE}_{k,h} = \begin{bmatrix} \text{MAE}_{1,1} & \text{MAE}_{1,2} & \dots & \text{MAE}_{1,H} \\ \text{MAE}_{2,1} & \text{MAE}_{2,2} & \dots & \text{MAE}_{2,H} \\ \vdots & \vdots & \ddots & \vdots \\ \text{MAE}_{K,1} & \text{MAE}_{K,2} & \dots & \text{MAE}_{K,H} \end{bmatrix}.$$

The MAE for each subset of climatic predictors ($\text{MAE}_{k,h}$) was calculated by averaging the subset-specific values across all time steps.

Model Predictions Under Climate Change. Cross-validated model outputs were used to generate spatially explicit predictions of dengue cases at a $0.5^\circ \times 0.5^\circ$ resolution for the periods 2050s and 2100. Model predictions were computed based on future climate and population scenario data. The predicted number of cases for a grid box was then multiplied by a factor of 11.5 to account for potential underreporting in the dengue data (56). We then evaluated changes in the number of dengue cases and in the length of the transmission season. The LTS was calculated from the predicted incidence rate per month. LTS = 1 for a given month if the predicted incidence rate per 100,000 people > 10 .

ACKNOWLEDGMENTS. F.J.C.-G., T.J.O., and I.H. received funding from the United Kingdom Government, Department for Business, Energy, and Industrial Strategy, as part of the implications of global warming of 1.5°C and 2.0°C project. F.J.C.-G., P.R.H., and I.R.L. were supported by the National Institute for Health Research, Health Protection Research Unit in Emergency Preparedness and Response at King's College London. C.A.P. and C.S.S.B. were supported by a Global Innovation Initiative grant.

- Messina J, et al. (2015) The many projected futures of dengue. *Nat Rev Micro* 13:230–239.
- Watts N, et al. (2015) Health and climate change: Policy responses to protect public health. *Lancet* 386:1861–1914.
- Campbell-Lendrum D, Bertollini R, Neira M, Ebi K, McMichael A (2009) Health and climate change: A roadmap for applied research. *Lancet* 373:1663–1665.
- Frumkin H, McMichael A, Hess JJ (2008) Climate change and the health of the public. *Am J Prev Med* 35:401–402.
- Caminade C, et al. (2014) Impact of climate change on global malaria distribution. *Proc Natl Acad Sci USA* 114:3286–3291.
- Piontek F, et al. (2014) Multisectoral climate impact hotspots in a warming world. *Proc Natl Acad Sci USA* 111:3233–3238.
- Ogden NH (2014) Estimated effects of projected climate change on the basic reproductive number of the Lyme disease vector *Ixodes Scapularis*. *Environ Health Perspect* 122:631–638.
- Bouzig M, Colón-González FJ, Lung T, Lake IR, Hunter PR (2014) Climate change and the emergence of vector-borne diseases in Europe: Case study of dengue fever. *BMC Public Health* 14:781.
- Colón-González FJ, Fezzi C, Lake IR, Hunter PR (2013) The effects of weather and climate change on dengue. *PLoS Negl Trop Dis* 7:e2503.
- Jansen CC, Beebe NW (2010) The dengue vector *Aedes aegypti*: What comes next. *Microbes Infect* 12:272–279.
- Rogers D, Randolph S (2006) Climate change and vector-borne diseases. *Adv Parasitol* 62:345–381.
- Watts D, Burke D, Harrison B, Whitmore R, Nisalak A (1987) Effect of temperature on the vector efficiency of *Aedes aegypti* for dengue 2 virus. *Am J Trop Med Hyg* 36:143–152.
- Murray C, et al. (2012) Disability-adjusted life years (DALYs) for 291 diseases and injuries in 21 regions, 2012 injuries in 21 regions, 1990–2010: A systematic analysis for the global burden of disease study 2010. *Lancet* 380:2197–2223.
- Shepard DS, et al. (2014) Approaches to refining estimates of global burden and economics of dengue. *PLoS Negl Trop Dis* 8:e3306.
- Garg P, Nagpal J, Khairnar P, Seneviratne SL (2012) Economic burden of dengue infections in India. *Trans R Soc Trop Med Hyg* 102:570–577.
- Bhatt S, et al. (2013) The global distribution and burden of dengue. *Nature* 496:504–507.
- WHO (2012) *Handbook for Integrated Vector Management* (World Health Organisation, Geneva), Report WHO/HTM/NTD/VEM/2012.3.
- Patz J, Martenad W, Focks D, Jetten TH (1998) Dengue fever epidemic potential as projected by general circulation models of global climate change. *Environ Health Perspect* 106:147–153.
- Jetten T, Focks D (1997) Potential changes in the distribution of dengue transmission under climate warming. *Am J Trop Med Hyg* 57:285–297.
- Hales S, deWet N, Maindonald J, Woodward A (2002) Potential effect of population and climate changes on global distribution of dengue fever: An empirical model. *Lancet* 360:830–834.
- Astrom C, et al. (2012) Potential distribution of dengue fever under scenarios of climate change and economic development. *Ecohealth* 9:448–454.
- Khormi HM, Kumar L (2014) Climate change and the potential global distribution of *Aedes aegypti*: Spatial modelling using geographical information system and CLIMEX. *Geospat Health* 8:405–415.
- Chan M, Johansson MA (2012) The incubation periods of dengue viruses. *PLoS One* 7:e50972.
- Brady OJ, et al. (2013) Modelling *Aedes aegypti* and *Ae. albopictus* survival at different temperatures in laboratory and field settings. *Parasit Vectors* 6:351.
- Goindin D, Delannay C, Ramdini C, Gustave J, Fouque F (2015) Parity and longevity of *Aedes aegypti* according to temperatures in controlled conditions and consequences on dengue transmission risks. *PLoS One* 10:e0135489.
- Reiter P (2001) Climate change and m-borne disease. *Environ Health Perspect* 109:141–161.
- Knutti R, Rogelj J, Sedlacek J, Fischer M (2015) A scientific critique of the two-degree climate change target. *Nat Geosci* 9:13–18.
- Victor D, Kennel CF (2014) Climate policy: Ditch the 2°C warming goal. *Nature* 514:30–31.
- Sedlacek J, Knutti R (2012) Half of the world's population experience robust changes in the water cycle for a 2°C warmer world. *Environ Res Lett* 9:448–454.
- UNFCCC (2015) *Adoption of the Paris Agreement (United Nations Framework Convention on Climate Change, Paris)*, Report FCCC/CP/2015/L.9/Rev.1.
- Schleussner C-F (2016) Differential climate impacts for policy-relevant limits to global warming: The case of 1.5°C and 2°C . *Earth Syst Dynam* 7:327–351.
- Osborn TJ, Wallace CJ, Harris IC, Melvin TM (2016) Pattern scaling using ClimGen: Monthly resolution future climate scenarios including changes in the variability of precipitation. *Clim Change* 134:353–369.
- Taylor KE, Stouffer RJ, Meehl GA (2012) An overview of CMIP5 and the experiment design. *Bull Am Met Soc* 93:485–498.
- Stehfest E (2014) *Integrated Assessment of Global Environmental Change with IMAGE 3.0. Model Description and Policy Applications* (PBL Netherlands Environmental Assessment Agency, The Hague), Report 735.
- Bhaskaran K, Gasparrini A, Hajat S, Smeeth L, Armstrong B (2013) Time series regression studies in environmental epidemiology. *Int J Epidemiol* 42:1187–1195.
- Hyndman RJ, Athanasopoulos G (2014) *Forecasting: Principles and Practice*. Available at <https://www.otexts.org/book/fpp>. Accessed August 12, 2014.
- Ebi K, Nealon J (2016) Dengue in a changing climate. *Environ Res* 151:115–123.
- Antonio FJ, de Picoli AS, Teixeira JVV, Mendes RdS (2016) Spatial patterns of dengue cases in Brazil. *PLoS One* 12:e0180715.

39. Barcellos C, Lowe R (2014) Expansion of the dengue transmission area in Brazil: The role of climate and cities. *Trop Med Int Health* 19:159–168.
40. Campbell LP, et al. (2015) Climate change influences on global distributions of dengue and chikungunya virus vectors. *Philos Trans R Soc B* 370:20140135.
41. Doolan DL, Dobano C, Baird JK (2009) Acquired immunity to malaria. *Clin Microbiol Rev* 22:1338.
42. Caminade C, et al. (2016) Global risk model for vector-borne transmission of Zika virus reveals the role of El Niño 2015. *Proc Natl Acad Sci USA* 114:119–124.
43. Villar L, et al. (2015) Efficacy of a tetravalent dengue vaccine in children in Latin America. *N Engl J Med* 372:113–123.
44. Scott LJ (2016) Tetravalent dengue vaccine: A review in the prevention of dengue disease. *Drugs* 76:1301–1312.
45. Capeding MR, et al. (2014) Clinical efficacy and safety of a novel tetravalent dengue vaccine in healthy children in Asia: A phase 3, randomised, observer-masked, placebo-controlled trial. *Lancet* 384:1358–1365.
46. Messina JP, et al. (2016) Mapping global environmental suitability for Zika virus. *eLife* 5:e15272.
47. Troyanskaya O, et al. (2001) Missing value estimation methods for DNA microarrays. *Bioinformatics* 17:520–525.
48. Perry PO (2009) *Bcv: Cross-Validation for the SVD (Bi-Cross-Validation)*, R package version 1.0. Available at <https://cran.r-project.org/web/packages/bcv/index.html>. Accessed June 13, 2017.
49. R Development Core Team (2010) *R: A Language and Environment for Statistical Computing* (R Foundation for Statistical Computing, Vienna).
50. Harris I, Jones PD, Osborn TJ, Lister DH (2014) Updated high-resolution grids of monthly climatic observations - The CRU TS3.10 dataset. *Int J Climatol* 34:623–642.
51. Hijmans RJ (2013) *Raster: Geographic Data Analysis and Modeling*. Available at [CRAN.R-project.org/package=raster](https://cran.r-project.org/package=raster). Accessed April 5, 2015.
52. CDO (2015) *Climate Data Operators*. Available at www.mpimet.mpg.de/cdo. Accessed March 12, 2017.
53. Jones B, Neill BCO (2016) Spatially explicit global population scenarios consistent with the Shared Socioeconomic Pathway. *Environ Res Lett* 11:84003.
54. Venables B, Ripley B (2013) *Modern Applied Statistics with S* (Springer, New York).
55. Wood SN (2006) *Generalized Additive Models: An Introduction with R* (Chapman & Hall/CRC, Boca Raton, FL).
56. Sarti E, et al. (2016) A comparative study on active and passive epidemiological surveillance for dengue in five countries of Latin America. *Int J Infect Dis* 44:44–49.